

Seismometer Theory

Preface

With all the confusion as to how a seismometer functions, one has to wonder if Einstein was the only one who ever acquired a complete conceptual mastery of inertia. His principle of relativity states that the "laws of physics remain the same for any non-accelerating frame of reference". In practical terms, this equivalence of inertial reference frames means that it is impossible to detect uniform motion on the basis of measurements conducted inside a box, such as a seismometer. Thus the only feature of motion having any importance whatsoever to an inertial seismometer is acceleration of the case that supports its mass M . It is very common to erroneously believe that any type motion of the case will be met with displacement of M relative to the case, because of the inertia of M . Be sure to understand that the only property of the motion that is "resisted" by M is the acceleration. Thus the acceleration is the most natural state variable with which to discuss measurements. For a pendulum as used in the VolksMeter, the displacement of the pendulum is at low frequencies directly proportional to the horizontal acceleration of the case, and thus is a direct measurement of the acceleration. Velocity and position, the other kinematic variables so frequently discussed in seismology, are readily inferred from the acceleration measurement.

As we shall see later, the output from a seismometer is directly proportional to acceleration, as long as the acceleration takes place at a frequency lower than the natural (eigen) frequency of the instrument, and additionally, it is operating with damping that is near critical. When the frequency of the drive is higher than the natural frequency of the instrument, the response of the instrument is attenuated by the ratio of the square of the drive frequency to the square of the eigenfrequency. If one is talking about the ground displacement, as opposed to the acceleration, just the opposite behavior is found. For those who want to believe that a seismometer responds directly to ground displacement, complete confusion results.

It is also important to note that the horizontal seismometer, such as a pendulum, responds to more than one type of acceleration. From "inside the box" of the instrument there is no way to distinguish between these two forms of acceleration, which are (i) horizontal acceleration of the instrument, and (ii) changes in orientation of the box (tilt) relative to the direction of the local field of the earth \mathbf{g} , having the magnitude of 9.8 m/s^2 . As a caveat to these comments, the following should be noted. If a rotation measurement is co-located with the seismometer, it is then possible to distinguish between tilt and horizontal acceleration. The number of observatories capable of this augmentation is at present vanishingly small.

The combination of a seismometer, clock, and recording device is referred to as a seismograph. Because the VolksMeter contains all these attributes, we will at times use the terms seismometer and seismograph interchangeably.

The simplest instrument to understand is that of a simple pendulum; i.e., a 'point' mass M hanging at the end of a flexible, inextensible string, as shown in Fig. 1.

1 Horizontal Seismograph

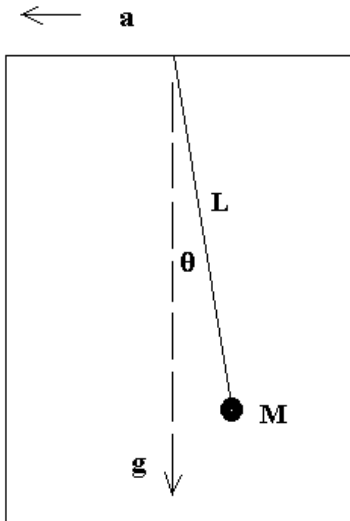


Figure 1 Illustration of the deflection of a pendulum in response to a constant horizontal acceleration of the case of the instrument. The mass movement (deflection) is in the opposite direction to that of the acceleration.

Here the direction of the earth's field is shown as the dotted-line vector \mathbf{g} . Its magnitude is 9.8 m/s^2 and if the acceleration were zero, then the angle θ would be zero (direction of a plumb bob) as opposed to the situation shown in Fig. 1 where $\theta = \tan^{-1}(a/g)$. Only a rare (huge) disturbance would ever invalidate the small-angle (radian) approximation $\theta \approx a/g$.

In Fig. 1 the deflection θ of the pendulum is constant because the acceleration is steady, and the acceleration can be simply estimated by measuring the deflection and using $a \approx g \theta$. Even if the acceleration is not constant, it can still be estimated by this same expression--if the frequency f of its variation is less than the natural frequency of the pendulum; which is given by $f_0 = (1/2\pi)\sqrt{g/L}$, and if the pendulum is damped close to the critical value so that oscillation is suppressed.

When a mechanical oscillator is disturbed by an acceleration, its response involves two parts: (i) an initial (transient response) at the natural frequency of the oscillator, and (ii) evolution toward entrainment with the drive. The duration of the transient is proportional to the Q of the oscillator, which is defined as $Q = 2\pi E/|\Delta E|$, where E is the total energy of oscillation, and $|\Delta E|$ is the loss in energy per cycle. The greater the damping, the smaller is Q , and the shorter is the transient. If $Q < 0.5$ then the oscillation is suppressed. Critical damping (transition between oscillation and no oscillation) occurs at $Q = 0.5$. Optimal performance of a seismometer is realized when the quality factor is close to but slightly less than critical.

2 Vertical Seismograph

The pendulum can only respond to horizontal acceleration; however a mass hanging from a spring, as shown in Fig. 2, will respond to vertical acceleration.

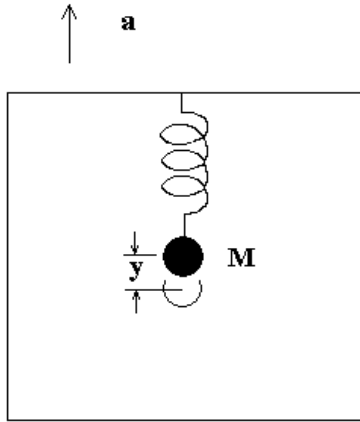


Figure 2. Illustration of a simplistic vertical seismometer. Horizontal motion is prohibited by means of mechanical constraints, and the mass displacement y is proportional to the constant acceleration a .

Whereas the pendulum is constrained against vertical motion by using an inextensible string, the mass in Fig. 2 is disallowed horizontal motion by means of mechanical constraints. Its displacement y , away from non-accelerated static equilibrium, is a measure of the ground's vertical acceleration via the relationship $a = ky/M$, where k is the spring constant, having units of Newtons per meter (N/m).

As before, the expression $a = ky/M$ can still be used to estimate the acceleration--if the frequency of drive f is small compared to the natural frequency of the mass-spring oscillator; which is given by $f_0 = (1/2\pi)\sqrt{k/m}$, and if the damping is near critical.

3 Sensitivity

An important design parameter for every seismometer is the mechanical part of its sensitivity to a low-frequency acceleration. For the vertical sensor this is defined as

$$\frac{y}{a} = \frac{M}{k} = \frac{1}{(2\pi f_0)^2} = \frac{1}{\omega_0^2} \quad (1)$$

and for the horizontal sensor it is

$$\frac{L\theta}{a} = \frac{L}{g} = \frac{1}{(2\pi f_0)^2} = \frac{1}{\omega_0^2} \quad (2)$$

It is thus seen that the mechanical sensitivity is proportional in either case to the reciprocal of the square of the natural frequency. Since an instrument's period is the reciprocal of its natural frequency in Hz, its sensitivity is proportional to

the square of its natural period in seconds.

4 Period-lengthening

The desire for high instrument sensitivity has nearly always been met in the past by efforts to lengthen the natural period of the instrument to as high a value as possible. In the case of the pendulum, this means using the largest convenient length L . In the case of the simple mass/spring, it means using the weakest spring (smallest value of k). For the simple system shown in Fig. 2, the height of the instrument becomes quickly prohibitively great, since the spring must support the mass against its weight Mg when in non-accelerated equilibrium. As k is decreased while holding M constant, the amount of equilibrium-stretch increases, and thus the height of the instrument must increase.

To lengthen the period of an instrument while simultaneously keeping its size small has always been a challenge. Some of the common methods to accomplish this are now described:

4.1 Garden-gate Horizontal Sensor

The favorite means for lengthening the period of horizontal seismometers has been to use the concept of the 'garden-gate', as illustrated in Fig. 3.

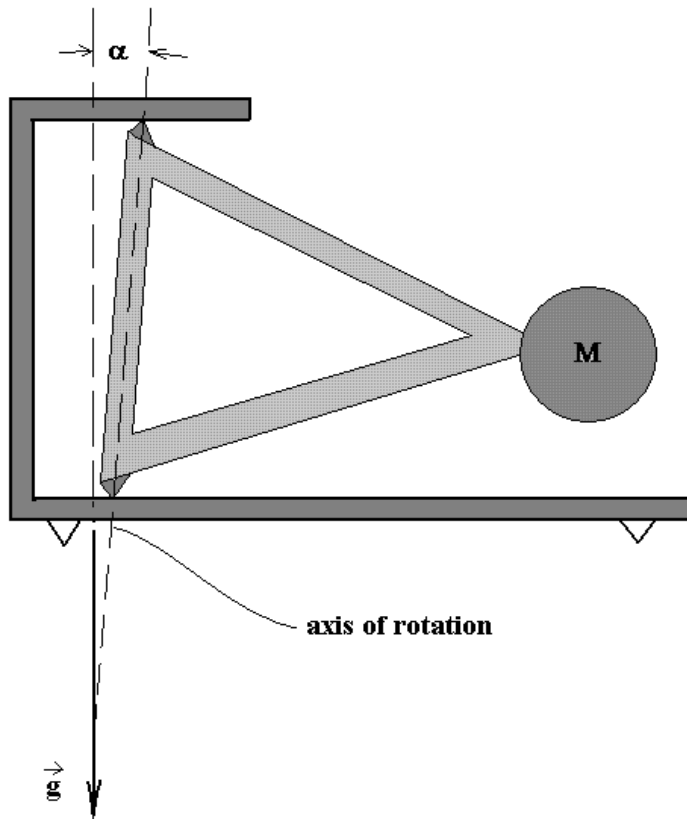


Figure 3. Illustration of a means for period lengthening of a horizontal seismometer. For this "garden-gate" instrument, acceleration in the direction perpendicular to the page results in a response.

Instead of a pendulum with a flexible 'string' to support M as shown in Fig. 1, one chooses a 'rigid' pendulum. This choice allows a configuration in which the axis of rotation can be positioned close to the vertical direction, as opposed to lying in the horizontal plane as in Fig. 1. In other words, the angle $\alpha \ll 1$ rad. What is essentially thus accomplished is a pendulum in which restoration is provided by means of an 'adjustable g '. Only the component of gravity given by $g \sin \alpha$ contributes to the period; i.e.,

$$T = 2\pi \sqrt{\frac{L}{g \sin \alpha}} \quad (3)$$

As $\alpha \rightarrow 0$ the period is seen to become very large for this hypothetical, ideal instrument. Real instruments are afflicted with anelasticity; where the prefix "an" means "other than". It is impossible to build a truly elastic system devoid of creep and the multiplicity of mesoscale complexities associated with it. Thus the practical maximum period of most garden-gate instruments (capable of performance without near-constant attention to keeping it operational) is about 30 s.

4.2 Folded-pendulum Horizontal Sensor

Another means for lengthening the period of a (hybrid) pendulum is to operate with a system comprising (i) an ordinary pendulum that is coupled to (ii) an inverted pendulum, as shown in Fig. 4.

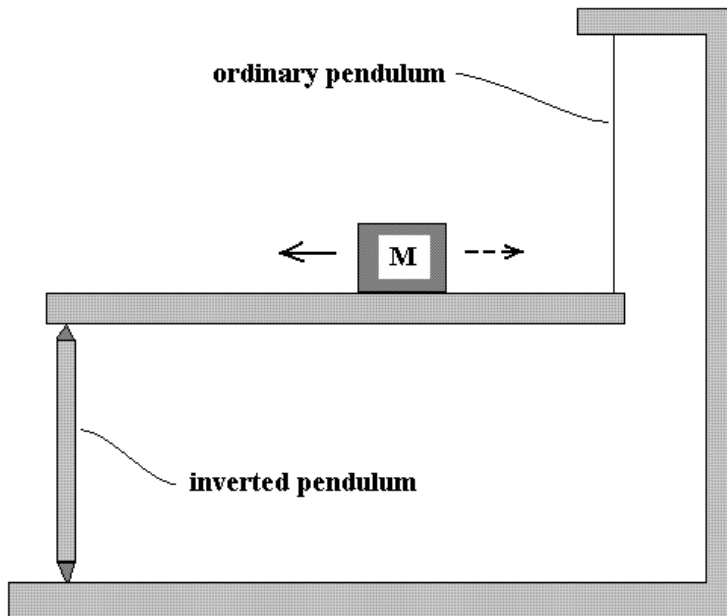


Figure 4. Illustration of another means for lengthening the period of a horizontal seismometer. Called a "folded-pendulum", this instrument responds to acceleration according to the directions shown by the arrows.

When the period of the inverted pendulum is adjusted close to that of the ordinary pendulum, the system can be made to oscillate with a much longer period than either pendulum alone. The influence of the inverted pendulum relative to the ordinary pendulum is controlled by the position of M on the horizontal boom. Moving the mass away from the ordinary pendulum causes the natural period to lengthen-until a position of unstable equilibrium is ultimately reached.

4.3 Inclined-Spring, Vertical Seismometer

Instead of operating with a vertical mass/spring system as shown in Fig. 2, the mass in this case is placed on one end of a horizontal rigid boom that is pivoted at the other end, as shown in Fig. 5.

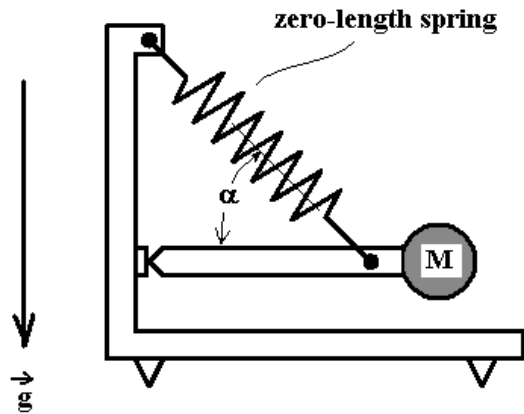


Figure 5. Illustration of a means for lengthening the period of a vertical seismometer.

The vertical member to which the pivot is attached also supports one end of the spring, and provision is made for the angle α between the spring and the boom to be adjustable. By this means the natural period can be adjusted. As α is decreased, the period lengthens.

4.3.1 Material limitations

The biggest problem with period lengthening is that the instrument is made to be not only more sensitive to acceleration (external influence), but also more sensitive to internal-influence changes; i.e., to the many imperfect properties of real-world materials. For example, real materials cannot be made to obey Hooke's law—the basis for the sensitivity estimate given above for the vertical sensor. Materials creep when stressed, due to defect structures; and they experience structural changes due to differences in thermal coefficients when the temperature changes. Although differences in thermal coefficients of expansion are one part of the challenge, the biggest single problem with springs is the temperature dependence of their spring constant k ; i.e., their thermal coefficient of the modulus.

Zero-length spring

Internal changes are significantly less influential for the inclined-spring vertical sensor shown in Fig. 5 when the spring is built according to the 'zero-length' concept. This idea was patented in the early 20th century by one-time physics-student Lucien LaCoste (University of Texas). The method of fabrication (one technique being to continuously twist the 'wire' while it is being coiled into a helix) results in a spring for which the force of restoration is proportional to the length of the spring.

5 Compromises

The performance of a seismometer depends on both (i) the mechanical structure, and (ii) the sensor and its electronics with which mass motion relative to the case is measured. In the early days of primitive electronics the best compromise was realized by strongly emphasizing the mechanical part of the design. Technology advances of the electronics industry in recent years are such that attention to sophisticated mechanical structures is no longer necessarily the best approach.

5.1 Electronics

5.1.1 First generation types—the Faraday-Law Detector

The earliest electronic detectors (in contrast to seismographs that generated records photographically) were those that operate on the basis of Faraday's law. With this method a voltage is generated by means of a time-varying magnetic flux in which a coil moves with the mass while positioned in the field of a magnet that is fixed relative to the case. The resulting voltage is amplified and then displayed (as on an ink-recording paper-helicord operating with a chopper-version potentiometric-type amplifier). It should be noted that the signal generated by this type of detector is proportional to the **time-rate** of change of mass position relative to the case. The time rate corresponds to the derivative of position, which according to the chain-rule of differentiation 'pulls out' a frequency multiplier term. The detector type is thus a 'velocity sensor'. It should be noted that what is measured by this sensor is not necessarily earth velocity, but rather the velocity of the inertial mass relative to its case. For frequencies of the earth motion that are lower than the natural frequency of the instrument—since the mass displacement is proportional to earth acceleration, the velocity sensor is actually measuring the 'jerk' of the earth. (The jerk is the derivative of acceleration.) On the other hand, for frequencies higher than the natural frequency, the sensor measures actual earth velocity.

As the acceleration drive frequency goes toward zero (very long-period), the output signal goes toward zero. Clearly, the way to avoid a degradation in low-frequency performance is to replace the velocity sensor with a position sensor. Because of the simplicity of the Faraday-law detector (not to mention tradition), many people have been reluctant to depart from velocity sensing, in spite of its serious low-frequency shortcomings.

5.1.2 Inductive-type detectors

The linear variable differential transformer (LVDT) has been used in many engineering applications. Nevertheless, transformers are fundamentally inferior to capacitive devices because of noises associated with their magnetic domains. The LVDT's were chosen instead of capacitive sensors for one primary reason-their output impedance is much lower than that of a typical capacitive sensor. Until the advent of high-impedance amplifiers, such as those of field-effect transistor type, it was difficult to avoid the severe signal attenuation that results when a capacitive detector is connected to an input stage with insufficient input impedance.

5.1.3 Capacitive-type detectors

Whereas the output signal from an inductive sensor depends on magnetic fields, the output signal from a capacitive sensor depends on electric fields. There are two common means for generating a voltage that depends on the state of the capacitor; either a change in (i) spacing between plates of the capacitor, or (ii) area common to capacitively-coupled plates.

The type of capacitive detector most common to seismometers is one in which two or more capacitors operate in concert while arranged in the form of a bridge as shown in Fig. 6.

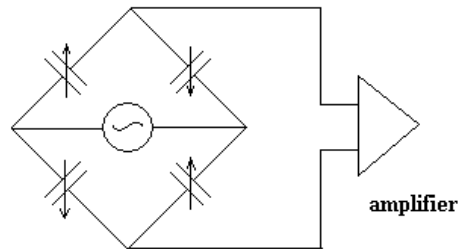


Figure 6. Schematic diagram of a bridge-type capacitive sensor. Shown is a fully-differential bridge in which all four capacitors of the bridge change in symmetric manner.

Until the development of the symmetric differential capacitive (SDC) sensor, all seismometers operating with capacitive detectors used a differential-capacitive architecture having lower symmetry than what is shown in Fig. 6. In this first-generation design, two of the oppositely changing capacitors would for such cases be fixed rather than varying. Alternatively, the fixed components could be inductors (secondaries of transformer windings, as a means for applying a stepped-up drive-voltage to the bridge.) As compared to the fully-differential capacitive structure, the earlier differential-capacitive sensitivity is reduced by at least a factor of two, assuming identical electrode areas and spacings. The gain from higher symmetry is typically more than two-fold for reason of the improved common mode rejection of the full- as opposed to half-geometry. It should be noted that linearity through bridge balance (sometimes called 'null') requires that the phase of the output signal relative to the drive signal must be employed. In other words, synchronous detection is employed-the heart of the lock-in amplifier invented by physicist Robert Dicke while at Princeton University.

6 Sensor geometry of the VolksMeter

For the VolksMeter, a position sensor was deemed essential, because of the design-goal to build an instrument with outstanding low-frequency capability. To the extent that temperature fluctuations of the electronics can be made inconsequential, the Volksmeter response to acceleration is independent of frequency for all drives satisfying the relationship $f < f_0$, all the way down to $f = 0$ (d.c.).

In consideration of the low-frequency goal, while studying the compromise between mechanical gain and electronics gain, it was determined that an area-varying capacitive detector was the only viable candidate. Highly-sensitive gap-varying capacitive detectors have a severely limited mechanical dynamic range, which makes them unsuitable for use as a position sensor. To manage the requirement enforced by the use of small gap-spacing, which is necessary for high sensitivity; commercial instruments employ force-balance by means of a feedback loop. This requires the addition of an 'actuator' with its associated sophisticated electronics, along with the gap-varying capacitive sensor. Thus the complexity, as well as the cost of the instrument, is greatly increased as compared to an instrument based on the architecture of the VolksMeter.

The design selected for the VolksMeter is illustrated in Fig. 7.

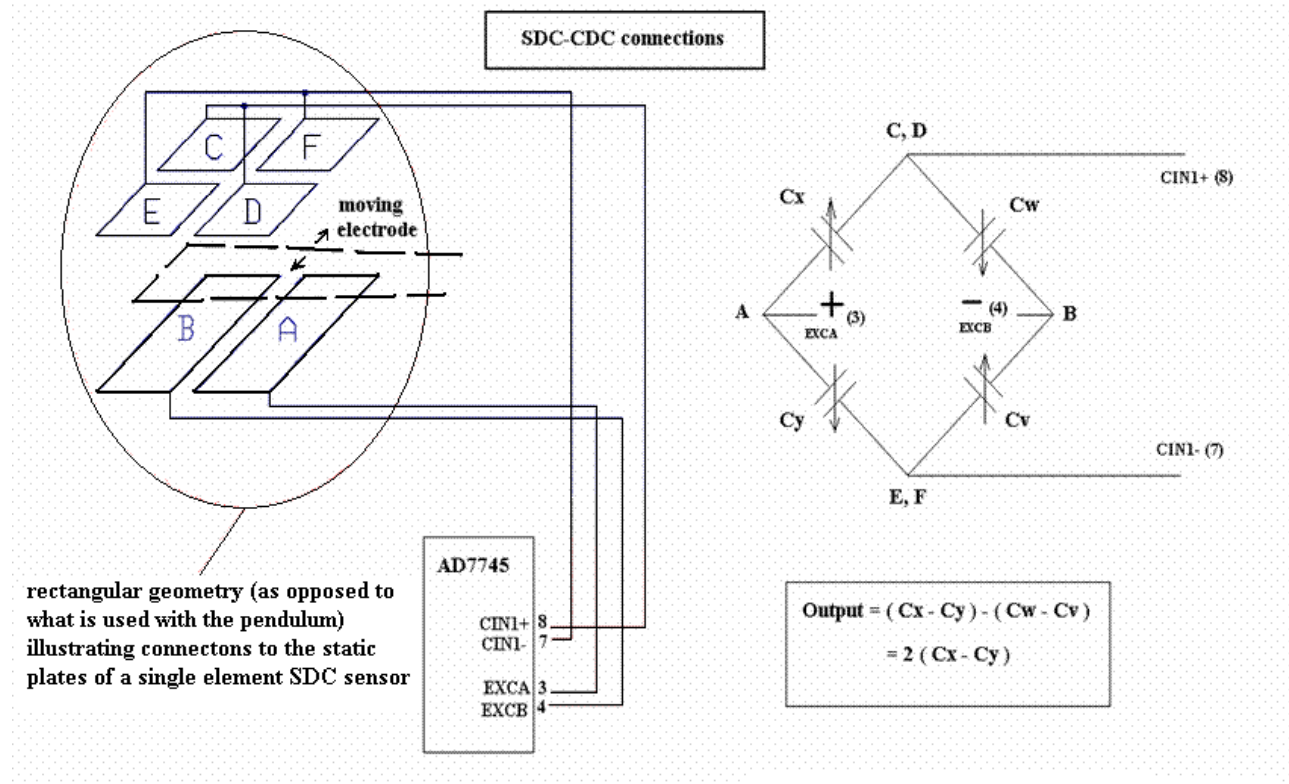


Figure 7. Schematic showing one element of the SDC array used by the VolksMeter. The heart of the electronics used with the array is Analog Devices' capacitance to digital converter (CDC), the AD7745 integrated circuit.

As noted by the comment in Fig. 7, only one element of the sensor array is shown. The array comprises eight elements, for reasons that are now explained.

It can be shown that the sensitivity of a single-element SDC detector is proportional to the inverse of the width of the moving electrode (dashed lines in Fig. 7)-if the output capacitance of the sensor (determined by means of the Thevenin equivalent circuit) were independent of this width. In fact, when the width of a single-element detector is reduced while keeping the length fixed; the sensitivity actually decreases--because the output reactance increases more rapidly than the ideal-system benefit. To eliminate this consequence of output capacitance decrease, several identical units are connected in parallel, configured to operate in concert. When the number of array-parts is inversely proportional to the width of a single-element moving electrode, then the output capacitance of the array is independent of the width parameter. Thus the improvement in sensitivity can be realized.

6.1 Mechanical dynamic range

Of course as the moving electrode width decreases, there is a resulting decrease in the maximum displacement of the pendulum that can be measured. The present design was tailored to the pendulum length and the need to insure sensor linearity. Reducing the width parameter results in loss of linearity because of fringe (edge) electric fields. Widths greater than roughly three times the gap spacing are nevertheless acceptable in this regard. The residuals from linearity are thus acceptably small and show a cubic relationship in the displacement. The width parameter of the VolksMeter was chosen so that the maximum-allowed mechanical motion of the pendulum corresponds to roughly two or three times the largest capacitance variation (8 pF) allowed by the CDC AD7745 chip.

7 Drive spectrum including the Pendulum Eigenfrequency

When analyzed on the basis of acceleration response, the simplest treatment of pendulum dynamics is for the case treated above, where the drive frequency is below the natural frequency of the instrument. As drive frequency approaches and goes above the natural frequency, things change because of the 'transfer function' T_F of the instrument. A true appreciation for how T_F influences pendulum response requires that one be familiar with all the state-variable descriptions that are commonly used.

The majority of seismologists were trained with mathematics that focused not on the acceleration, but rather as a starting case, on the displacement of the pendulum. Thus we provide the details of that case before discussing the intricacies of transfer functions. The equation of motion for the pendulum is given in the model section of this manual, which we reproduce here:

$$\ddot{\theta} + \frac{\omega_0}{Q} \dot{\theta} + \omega_0^2 \theta = -\frac{\omega_0^2}{g} a(t) = -\frac{\omega_0^2 \omega^2}{g} A_G \quad (4)$$

where $a(t)$ is ground acceleration, related simply to ground displacement amplitude A_G for steady state motion. The distance from the axis of the pendulum to the center of percussion, designated L_P , is the best parameter with which to specify pendulum displacement in nanometers as opposed to angular displacement in radians. The reader who would apply dimensional analysis to these results for purpose of checking validity-must be careful to recognize that the radian is a 'non-unit' unit; i.e., it is actually a dimensionless quantity according to the definition of radian angle measure. If we let $x = L_P \theta$, then the pendulum displacement x (system international units of meter) obeys the following equation:

$$\ddot{x} + \frac{\omega_0}{Q} \dot{x} + \omega_0^2 x = -\frac{L_P \omega_0^2 \omega^2}{g} A_G \quad (5)$$

It should be noted that the damping coefficient (which is referred to as linear viscous) is here shown as ω_0/Q . Few people other than physicists use this form; more commonly in physics textbooks the term multiplying the velocity $[x\dot{t}]$ is replaced by 2β , where $e^{-\beta t}$ describes the exponential envelope of the turning points of the pendulum motion when oscillating in free-decay. Thus the relationship between Q and β is $Q = \pi/(\beta T)$ where T is the natural period of the pendulum; i.e., $T = 1/f_0$. In the seismology world, the most common damping parameter b is defined such that $Q = 1/(2b)$.

Much is made of the 'damping redshift' (period longer with damping than without), so that one might want to argue for a subscript zero on T . In fact, real pendulums do not obey the linear equations being here used with sufficient accuracy to warrant attention to such arguments. Even if measurable (only with great difficulty), the redshift is irrelevant to present discussions. Part of the reason for Q being the superior means for specifying damping is that it has no variants when expressed canonically (as defined in this document). On the other hand 'damping coefficients (which are not really constant, but depend on frequency in real systems) take on a variety of different forms. For example the logarithmic decrement (βT) is frequently used to specify the damping.

The steady state solution to Eq.(5) is given by

$$\frac{x_0}{A_G} = \frac{\omega_0^2 L_P}{g} \frac{\omega^2}{[(\omega_0^2 - \omega^2)^2 + \omega_0^2 \omega^2 / Q^2]^{1/2}} \quad (6)$$

where x_0 is the amplitude of the pendulum displacement at angular frequency $\omega = 2\pi f$. It is instructive to look at Eq. (6) in the case of a simple pendulum; i.e., one in which $L_P \rightarrow l$ is simply the length of the string supporting a point mass.

For this simple pendulum $\omega_0^2 = g/l$, and so

$$\frac{x_0}{A_G} = \frac{\omega^2}{[(\omega_0^2 - \omega^2)^2 + \omega_0^2 \omega^2 / Q^2]^{1/2}} \quad (7)$$

In the limit of $\omega \gg \omega_0$ the pendulum displacement is seen to equal the ground displacement. On the other hand, in the limit as $\omega \ll \omega_0$ one obtains

$$x_0 = \frac{\omega^2}{\omega_0^2} A_g, \quad \omega \ll \omega_0 \quad (8)$$

7.1 Transfer Functions

As the drive frequency approaches and goes above the eigenfrequency, then the acceleration response of the pendulum starts to decrease in accord with the graph shown in Fig. 8.

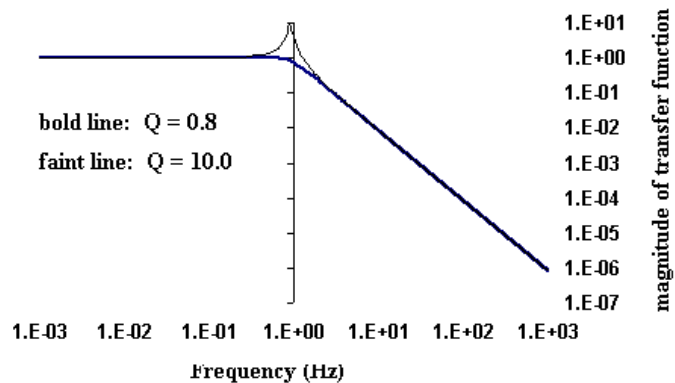


Figure 8. Transfer function T_F for the response of a pendulum to horizontal acceleration. The curve is based on the classical dynamics of a viscous-damped simple harmonic oscillator.

The seismometer operates with eddy-current damping provided by rare-earth permanent magnets, so that the quality factor is in the vicinity of $Q = 0.8$. Critical damping at $Q_c = 0.5$ would not yield quite so optimal a transition through the eigenfrequency value $f_0 = 0.918$ Hz.

The faint-line response is for a hypothetical instrument having a much larger quality factor. Such an instrument is not generally useful because of the long time required for transients of the pendulum to decay, following a change in drive amplitude or frequency. Such transients do not allow a simple means to deconvolve the drive contribution from the total response. When operating with a Q near the critical damping value, the pendulum entrains to the drive quickly, so that the response is a faithful representation of ground acceleration (once corrected for the influence of the transfer function).

7.2 Amplitude and velocity response

Except for strong-motion instruments, seismologists usually represent earth motion with a display that is based on a state variable other than acceleration (units of m/s^2). Other possible representations of earth motion versus time include position (m), and velocity (m/s). (Usually the $\mu m = 10^{-6}$ m is instead employed because of the small displacements observed.) As noted, however, acceleration is foundational and the use of these other variables is a source of confusion for many.

To convert among the different types of representation, one employs the very means with which the specific power was estimated above. As noted or implied, acceleration is the derivative of velocity and velocity is the derivative of position. Thus velocity is obtained from acceleration through division by omega, and position is obtained from velocity also through division by omega.

Thus the transfer functions for the response of a pendulum to earth displacement are easily understood in relationship to the curve of Fig. 8. The fall-off in Fig. 8 goes as $1/\omega^2$ when $f > f_0$. Since acceleration is proportional to ω^2 times position, the curve must be independent of frequency above f_0 and fall-off as ω^2 below f_0 as shown in the left graph Fig. 9. The right graph shows the transfer function for the response to velocity.

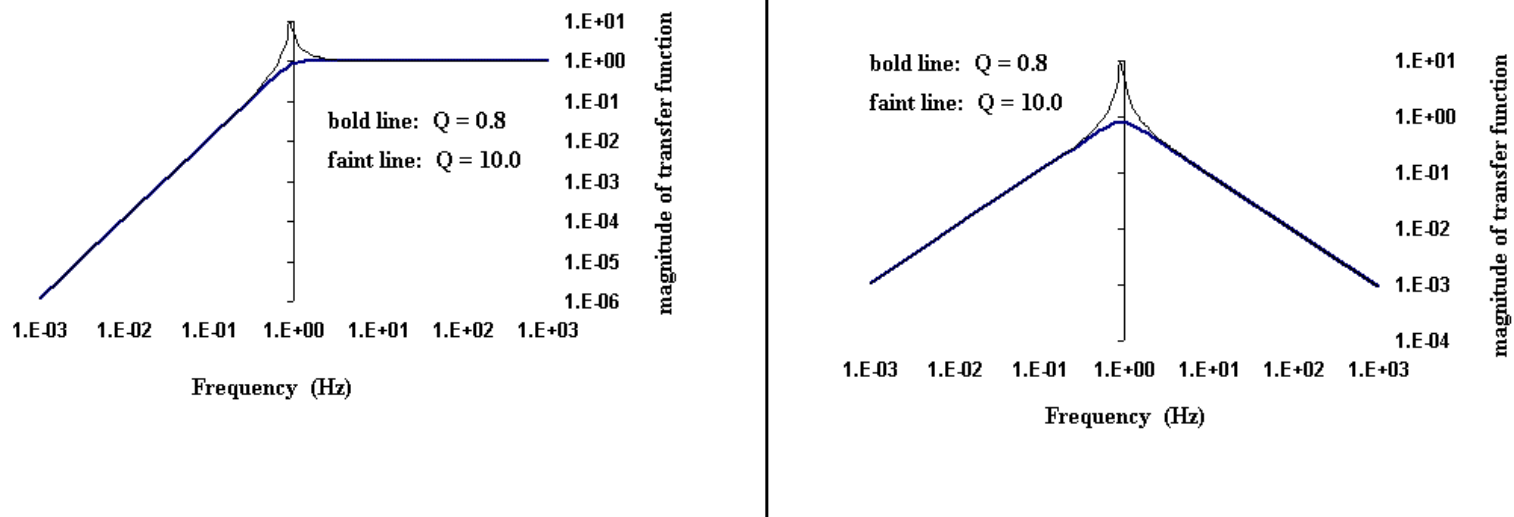


Figure 9. Transfer functions for the response of a pendulum to horizontal components of ground motion- position (left graph) and velocity (right graph).

It is worth noting that the transfer functions shown in figures 8 and 9 for the pendulum are identical to those describing the behavior of a spring-seismometer, except with the state variables corresponding to vertical as opposed to horizontal earth motions.

8 Power

Every sensor, no matter the type, responds to the stimulus that excites it according to one thing only- energy transfer (the time rate of energy being the power)- a statement that is not in conflict with the earlier comment of this document, that inertial seismometers respond only to acceleration. We now provide a means for estimating the fraction of the total oscillatory power of the earth that lies in a given frequency range to which the VolksMeter is able to respond.

Consider a mass element m of the earth that oscillates in steady state. We know the amplitude of its acceleration to be $a_0 = g \theta_0$ for frequencies of oscillation that are below the natural frequency of the VolksMeter. Since the velocity of the mass is simply the acceleration divided by the angular frequency, one obtains the following expression for the total oscillatory energy of this mass:

$$E = \frac{1}{2} m v_0^2 = \frac{1}{2} m \frac{g^2 \theta_0^2}{\omega^2} \quad (9)$$

Dividing this energy by the period $T = 2\pi/\omega$ gives a value of oscillatory power. A correction to this value is necessary for the following reason. Power balance involving the generation of heat is central to our discussion. If the earth could oscillate without damping, then no amount of external energy input would be needed to keep it oscillating. Similarly, if a seismometer were to operate without damping, no input of energy from the earth would be necessary to keep it moving. Of course damping is part of the dynamics of both systems. The damping of the instrument that monitors the earth is easy to describe in terms of the balance between power in and energy out per second in the form of heat. As noted earlier, the quality factor is defined as $Q = 2\pi E/|\Delta E|$ where E is the total energy and $|\Delta E|$ is the loss of energy per cycle. When operating with critical damping ($Q = 1/2$), we see that the power that is converted to heat is a factor of 4π greater than the value that would be estimated on the basis of Eq. (9). We thus choose the following expression for the specific power (power per unit mass):

$$P = \frac{g^2}{2\pi f} \theta_0^2, \quad f < f_0 \quad (10)$$

A completely proper accounting for the power would have to consider every term in the frequency dependence of the Q of the earth, which is a hopefully complicated task. For persistent oscillations (fairly high Q eigenmodes) Eq. (10) is insufficient; but for most of the broadband noise of the earth it is a reasonable starting point for understanding how the oscillatory power of the earth is distributed among the frequencies allowed by its density of states.

Let us illustrate our discussion with an example. Consider the response of the VolksMeter to an idealized Rayleigh (surface) wave that is monochromatic, having a period of 1000 s. To say that it is monochromatic implies a high Q , so the use of Eq.(10) is questionable insofar as physical meaning, but let us go ahead and use it for purpose of illustration.

The frequency of this wave,

at $f = 1$ mHz, is nearly three orders of magnitude lower than the natural frequency of the instrument, $f_0 = 0.92$ Hz. If our instrument were to use a velocity-type rather than position-type sensor, then the output signal in response to this wave would be nearly three orders of magnitude (1000 times) smaller.

The seismometer responds only to the horizontal component of the wave; because ground particle motion of a Rayleigh-wave is elliptical, there are both horizontal and vertical acceleration components. In the discussion of pendulum dynamics (appendix) of this manual, the response of the pendulum is given, and we use that result here to obtain

$$a_0 = g \theta_0 \frac{[(\omega_0^2 - \omega^2)^2 + \omega_0^2 \omega^2 / Q^2]^{1/2}}{\omega_0^2} \rightarrow g \theta_0 \quad \text{for } \omega \ll \omega_0 \quad (11)$$

So there is no transfer function correction necessary for this Rayleigh wave case, because of its low frequency. In section 9 that follows, where higher frequencies are considered, the correction due to T_F will be included.

A typical value for the calibration constant for a pendulum of the VolksMeter is 2.5×10^9 counts per radian (2.5 Gcts/rad). If we assume that the indicated Rayleigh wave results in a sensor output amplitude of 50 counts (20 nrad), then the average specific power of the horizontal component of the wave [one-half of the value calculated from Eq. (10)] is estimated to be $P = 3.06 \times 10^{-12}$ W/kg.

The conventional means for specifying any quantity having a broad range of values, is to work with the decibel. Thus we take the logarithm (base 10) of the estimate and multiply the result by 10. If we were working with amplitude A rather than power, then the log of the amplitude (properly referenced) would be multiplied by a factor of 20, since $P \propto A^2$ (recognizing the exponent property of the log function). Thus the indicated specific power yields the result -115 dB. Since the units of P are W/kg, the dB values are referenced to $\text{m}^2/\text{s}^3 = \text{m}^2 \text{s}^{-3}$.

It is instructive to also consider the estimated amplitude of the ground motion associated with this Rayleigh wave. It is given by $A = (g/\omega^2)\theta_0$, which yields the value 5.0 mm. At the position of the VolksMeter sensor, the amplitude of pendulum motion due to this earth disturbance is dramatically smaller by a factor of roughly $0.3 \times (\omega/\omega_0)^2 = 10^{-6}$; i.e., it is moving only about 5 nm.

9 Power Spectral Density PSD

A state variable (position, or velocity, or acceleration) versus time is what gets displayed real-time from the output of seismometers. Information in the frequency domain provides auxiliary information that is of great value in trying to understand the dynamics of what is observed. Generally, earth motions are distributed in a largely smooth manner over a broad frequency range. An ideal seismometer would respond to every spectral component in the same manner; i.e., like the Fig. 8 curve for $f < f_0$. Unfortunately, there is no broadband instrument of ideal type. All instruments have a corner frequency specified by f_0 . It is possible by electronic means using force feedback to alter the f_0 of a seismic element. Such feedback is also used to establish the near critical-damping required of the element. Regardless, practical instruments are always characterized by something very much like one of the three transfer functions shown in figures 8 and 9.

The best means for optimizing a broadband instrument is to consider the spectral character of the noise it generates independent of any external stimulus. For instruments other than those of force balance type, the Noise Equivalent PSD is readily obtained by caging ('locking') the pendulum to prevent it from moving in response to earth accelerations. When not caged, the same technique is used to generate PSD's that illustrate earth motion (assuming the results are everywhere larger than the threshold density values established by instrument noise. If the signals from the electronics generated by earth motions are everywhere in frequency below the instrument's Noise Equivalent PSD values; then there is no way any of the earth motions can be detected (except perhaps by considering the correlated response of two different instruments). Obviously then, the primary objective in instrument design, is to try and decrease the instrumental noise equivalent PSD to the lowest possible value everywhere.

The 'workhorse' for generating the PSD is the Fourier transform, which is of the fast type (FFT originated by Cooley and Tukey). The FFT spectrum is routinely calculated by most software programs used by seismologists, both professional and amateur. It should be noted, however, that not all algorithms in common use are properly normalized. An easy test of normalization is to look at the 'intensity' of a spectral line corresponding to a monochromatic signal. If as commonly happens, the calculated intensity increases in direct proportion to the time duration of the signal, then the algorithm is not normalized.

As compared to the PSD, the value of the FFT is limited because it is 'instrument dependent' through the transfer function T_F of the seismometer. This dependence is removed in the calculation of the PSD for the VolksMeter, according to the following set of equations:

$$T_F = \frac{f_0^2}{\sqrt{(f^2 - f_0^2)^2 + \frac{f^2 f_0^2}{Q^2}}},$$

$$f_0 = 0.92 \text{ Hz}, \quad Q \approx 1/2$$

(12f)

$$P = 10 \log \left(\frac{g^2 FFT_{mag}^2}{2\pi f C_c^2 T_F^2} \right) + 10 \log \left(\frac{f}{f_{min}} \right),$$

$$g = 9.8 \text{ m/s}^2, \quad C_c = 2.5 \times 10^9 \text{ counts/rad}$$

In this expression P for the specific power spectral density, the FFT magnitudes as a function of f (twice the square root of the sum of the squares of real and imaginary components) are available from WinQuake by 'exportation'. The reason for multiplying the sum of the squares by a factor of two involves an inherent 'degeneracy' of the FFT processing. Negative frequencies are part of every Fourier transform operation; and their contribution to the power equals that of the positive frequencies. Since the negative terms are not explicitly included in the representation, one must double all the components to get the correct result.

The term f_{min} corresponds to the lowest frequency value generated by the FFT algorithm; it is established by the Nyquist frequency, which equals one-half the sampling rate. This minimum frequency is equal to the Nyquist frequency divided by one half the number of points used to generate the FFT.

It turns out that the PSD values calculated by the indicated expression for P in equation set (12) correspond closely to watts per kilogram per one-seventh of a decade. This is convenient since the density 'bin-width' of one-seventh is also commonly employed to specify earth noise (work of Jon Berger et al). The width of such a bin straddling the frequency f , is for this case defined as

$$10^{\log f - 1/14} \text{ to } 10^{\log f + 1/14} \quad \rightarrow \quad f / 1.1788 \text{ to } 1.1788 f \quad (12)$$

The indicated expression for the PSD is general and could be used for other seismometers using a position sensor, apart from the VolksMeter-specific numbers indicated for f_0 and C_c .

An illustration of the great influence that the transfer function has on the spectrum at higher frequencies is provided by Fig. 10.

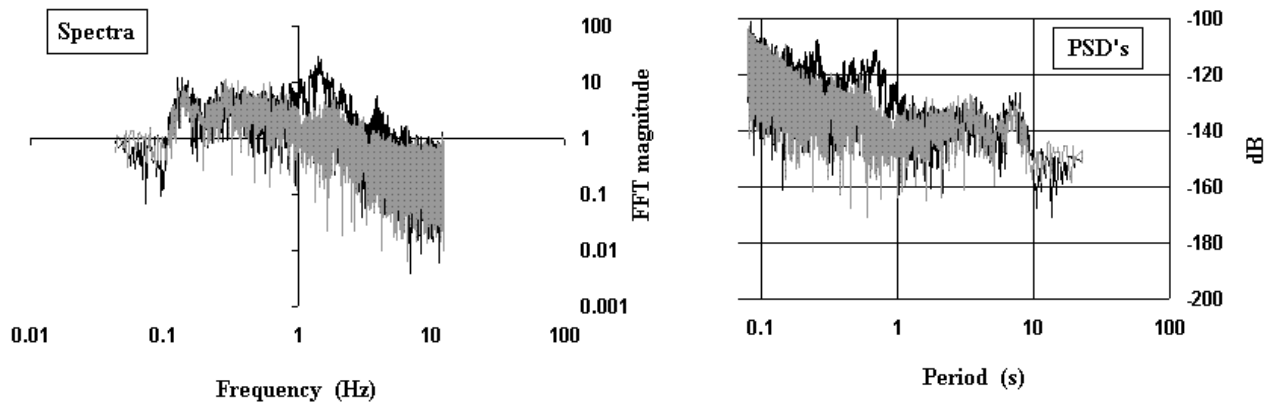


Figure 10. Comparison of (i) spectrum to (ii) PSD generated from a record of 600 s duration, containing a small local earthquake (Mag. 3.1, 75 km away). The faint curves represent the background, computed from another 600 s record taken 1-h later. The dB values of the PSD are relative to $\text{m}^2 \text{s}^{-3}$ per 1/7 th decade. Unlike the PSD curves, for $f > f_0 = 0.918$ Hz, because of the fall-off in acceleration-sensitivity of the pendulum, the spectrum is not a faithful representation of the distribution of ground motion power.

A graph-type that is commonly used (and equivalent at least in shape to Fig. 10) is specified as having units of m^2/s^4 per Hz. These units are not compatible with a statement of power. The closest thing in the popular literature to PSD's with properly labeled axes are the earth noise graphs generated by Jon Berger and P. Davis [J. Geophys. Res. Vol. 109, B11307 (2004)]. Shown in Fig. 11 is a graph for horizontal earth noise, taken from their paper.

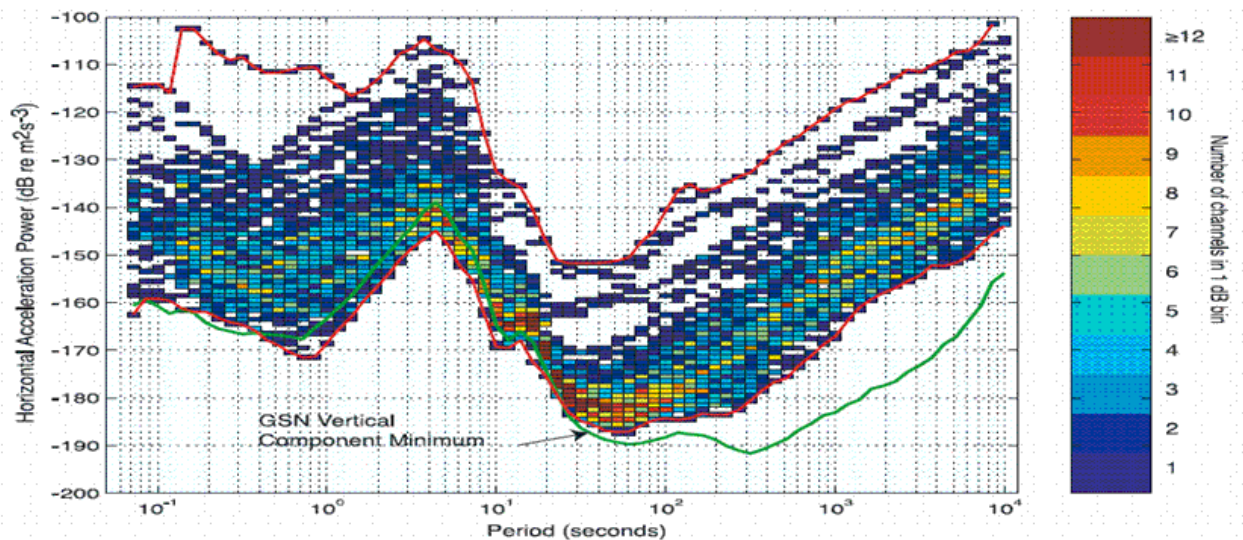


Figure 11. Plot of 'Horizontal acceleration power' from the paper by Berger et al. The spectral density bin-width for their data is 1/7 th decade.

The reader should pay special attention to the fact that we choose to specify spectra as a function of frequency; however, specific power spectral density is specified as a function of period. The primary reason for the latter choice is because of the similarity in trend of PSD's to similar graphs of earth noise, that are plotted versus period. Notice the similarity of the PSD of Fig. 10 and the data of Fig. 11 in the range from 0.08 s to 20 s. The primary difference is that the microseism 'peak' of Fig. 10 is a 'double hump'.

The difference between the FFT and the PSD can be more fully appreciated by considering the difference between intrinsic and extrinsic quantities of engineering type. For example the spring constant k that relates force and displacement of a Hooke's law spring is an extrinsic parameter; i.e., it depends on the size of the spring. The modulus that relates stress to strain for the spring is an intrinsic parameter. Being independent of spring size, it depends only on the material from which the spring is fabricated.

Shown in Fig. 12 is the VolksMeter's noise equivalent PSD (darker curve). Also shown is how this curve would change if the sensor used were of velocity-type rather than position-type.

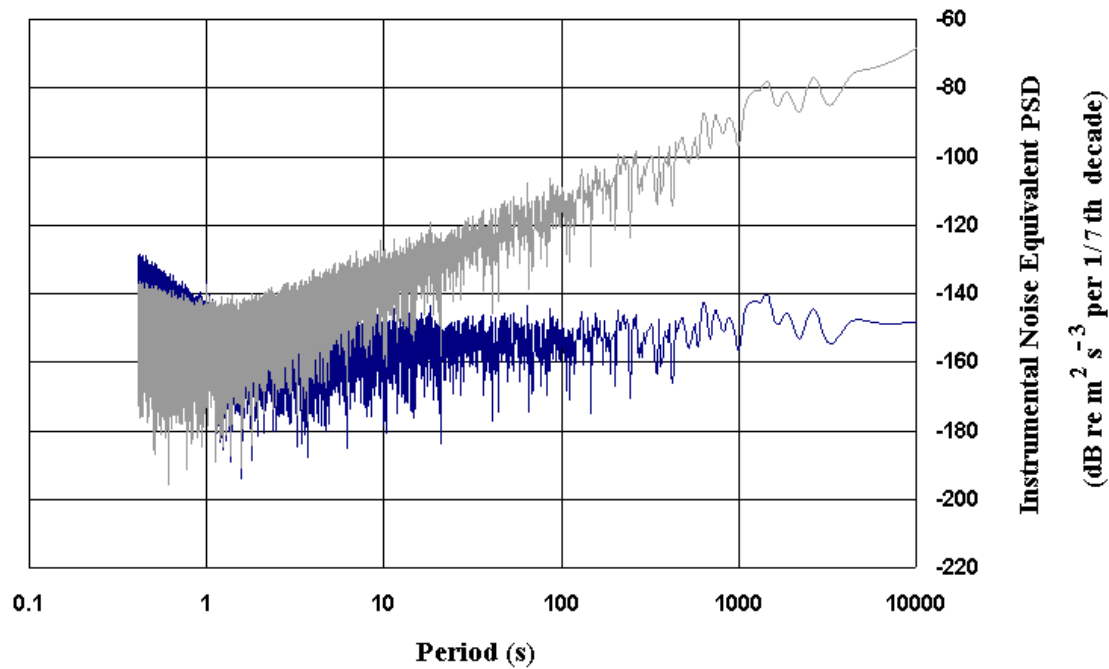


Figure 12. Illustration of the dependence on sensor-type of an instrument's noise equivalent PSD. The fainter curve corresponds to the velocity sensor.

The most important thing to recognize from a comparison of the two graphs of Fig. 12 is the following: for all else being equal, (i) above the corner frequency (short periods) a velocity sensor will outperform a position sensor, but (ii) below the corner frequency (long periods) a position sensor will outperform a velocity sensor. Because of the increasing importance to seismology of low-frequencies, it should be clear to the reader why a position sensor was chosen for VolksMeter use.

The TRUE PSD is a powerful tool for understanding many of the complex features of our planet. The VolksMeter is unique in its use of this tool that has not been previously exploited. In other parts of this manual some examples of its use are provided.

Erroneous labels of PSD

Observe from the PSD expression in Eq.(12f) that it is possible to rewrite the formula as

$$P = 10 \log \left(\frac{g^2 \text{FFT}_{\text{mag}}^2}{2\pi f_{\text{min}} C_c^2 T_F^2} \right) \quad (13)$$

This means that at least the proper shape of the PSD can be realized by simply (i) correcting for the transfer function, and then plotting on a log scale the squares of the Fourier component magnitudes corresponding to acceleration. Because the square of the acceleration is in m^2/s^4 , this is the reason, no doubt, that the "standard" (erroneous) label for the ordinate of these graphs is indicated as $\text{m}^2/\text{s}^4/\text{Hz}$. Such expressions can never be consistent with (specific) power spectral density because the PSD can ONLY have units of m^2/s^3 per some density interval such as 1/7th decade. Evidently, what the "standard" plot really represents is $\text{m}^2/\text{s}^3/\text{decade}$ (or fraction of a decade determined by constants employed) rather than $\text{m}^2/\text{s}^4/\text{Hz}$.

Graphics Subtleties

There are a number of differences in the proper representation of the PSD, depending on how the function gets graphed. A proper display must account for the fact that the function is a *density*. As such, the ordinates of the graph must be watts per kilogram per 'density type'. The density type can be (i) Hz for a frequency plot, (ii) s for a period plot, or (iii) decade or fraction thereof of either frequency or period. One could also of course substitute octave for decade.

For data that has been generated by the FFT, the bin-width necessary to properly account for that fraction of the total power that is assigned to the bin- is independent of the abscissa variable for one and only one case- that of linear frequency. The reason is that the discrete components of the Fourier transform approximated numerically by the FFT, are separated from each other by the fixed width $\Delta f = f_{\text{Nyquist}}/(N/2)$, where N is the total number of points used in calculating the FFT. A sum over all the components, when multiplied by Δf approximates the total power, because it represents the integral over the frequency domain. Parseval's theorem says that this must equal the same integral over all points in the time-domain.

If one were to plot the PSD in terms of linear period instead of linear frequency, where $T = 1/f$, a correction factor would be necessary; since the differentials of frequency and period are related as follows:

$$dT = -\frac{1}{f^2} df = -T^2 df \quad (14)$$

Because df is constant for the FFT components, a proper accounting for the power in this case must consider the quadratic dependence on T of dT . Figure 13 illustrates the dramatic influence of the T^2 feature on the linear-period graph. In these and also the graphs that follow, the data (represented by the dots) is not connected by lines in the usual manner. The difference in graph dot-densities (and thus power densities) for the two plots is dramatic. Unlike its constancy in the right-side graph, there is a dramatic decrease of density with lengthening period in the left-side graph.

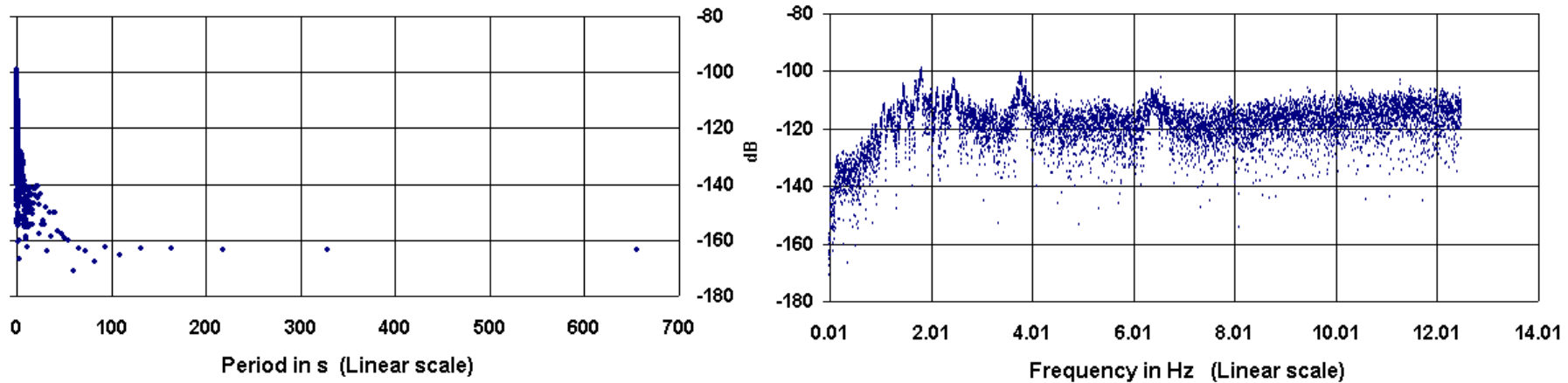


Figure 13. Illustration of the differences between a PSD (from VolksMeter data that recorded an earthquake) plotted versus period in the left graph (linear scale) and plotted versus frequency in the right graph (linear scale).

Neither the linear frequency case nor the linear period case is commonly used. Rather, scales involving the log of frequency or log of period is the preferred representation. Because of the abscissa 'compression' that results from using the log scale, one has the following issue to consider:

$$d \log f = df / f \quad \text{and} \quad d \log T = dT / T = -T df = -df / f \quad (15)$$

where the natural log is used for its simpler math (different from base 10 of other graphs only by the constant 0.4343 or its inverse). What then is the consequence of plotting versus frequency with a log scale or of plotting versus period with a log scale? The answer is: as frequency increases in a log plot, the df required to keep constant the 'weighting' factor that is part of proper accounting for the power must be increased. More specifically, the bin-width must be made proportional to the frequency. This explains why the term $10 \log (f/f_{\min})$ has been added to the PSD expression in Eq.(12f).

There is no difference to the weighting factor when working with period as a log-scale. One may simply plot the same ordinate values versus the reciprocal of the frequency (period) using a log-scale for the reconfigured abscissa values. The two curves are mirror images of each other, as illustrated in Fig. 14.

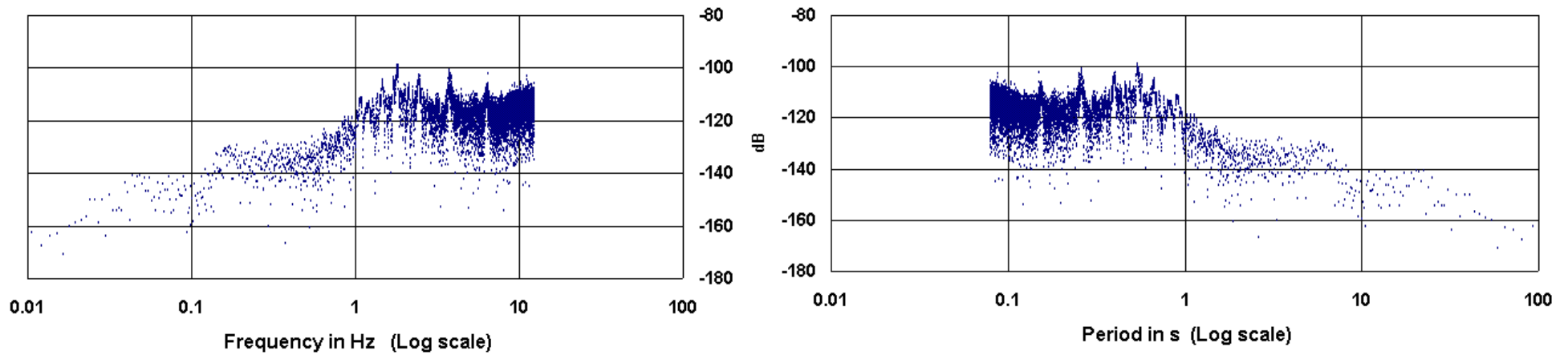


Figure 14. Illustration of the symmetry between PSD's plotted with a log-scale involving frequency (left graph) and period (right graph). The 'dot-density' that represents 'power density' is readily seen to be greater at high frequencies (short periods) than at low frequencies (long periods).

10 Cumulative Spectral Power CSP

The VolksMeter has been used to generate another power function of spectral type that appears not to have been previously considered for use with seismic data. Like the PSD, its generation using Excel is both (i) straightforward, and (ii) results in a new tool to assist our better understanding of the earth. As suggested by features in the examples that follow, the CSP could allow for better earthquake modelling. There is even a tell-tale indicator of the possibility of some degree of earthquake forecasting. Only extensive future data of the preliminary type that is here presented will determine whether the CSP might indeed show precursors to large earthquakes.

So what is the CSP? Before describing the particulars of how it is calculated, let us note the similarity of the PSD/CSP to two math functions routinely used in probability theory. These are the (i) probability density function pdf, and (ii) cumulative probability function cpF. The pdf is simply the derivative of the cpF, and the cumulative form is usually considered the more fundamental of the two. The cpF starts at a low value (zero) and rises without dipping to a maximum value (unity)

The CSP is obtained by integrating the PSD from the lowest frequency component considered in the FFT up to the frequency corresponding to the specified value of the abscissa. Instead of using the frequency for the independent (abscissa) variable of the graph, we choose to work instead with the period, as has been done with the PSD. Examples are provided by the set of five curves shown in Fig. 15.

Cumulative Spectral Power (Integral of PSD from 2.8 s to Period value (abscissa))
 (grn = 30 Mar, red = 31 Mar, blk = 1 Apr, gray = 2 Apr, blue = 3 Apr)

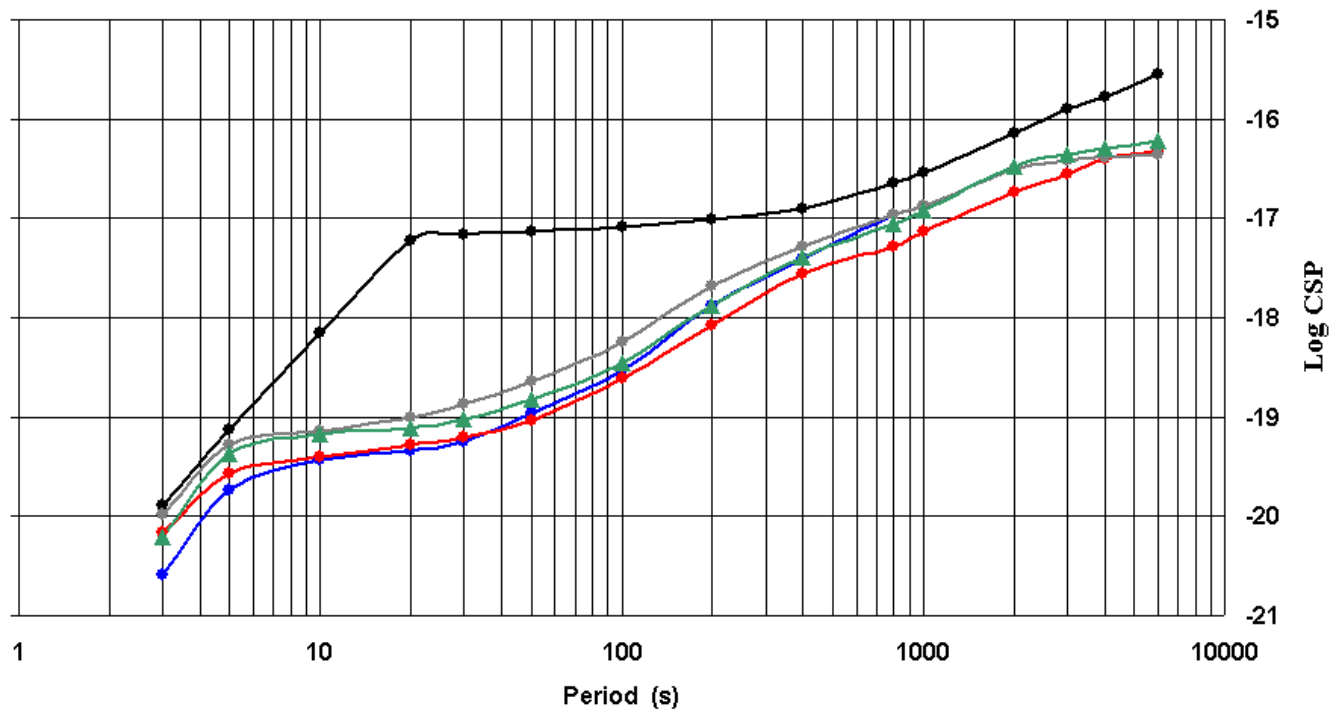


Figure 15. Five CSP graphs generated from 12 hour-duration individual records at the same time, but on days that straddle the Solomon Islands earthquake of 1 April 2007.

Probably the singlemost important advantage of the CSP over the PSD involves noise. Because the CSP involves the integral of the PSD, there is an inherent noise reduction associated with its generation. Because spectra are inherently noisy, the CSP is dramatically smoother than the PSD. If the Fig. 15 graph were constructed with their associated PSD curves, instead of the CSP curves shown; then very little difference could be realized visually except that the earthquake curve (black) would be separated significantly from those of the other four days.

The simple shape of the CSP curve corresponding to 1 April is startling. Simplicity is the hallmark of successful physics representations, and this curve suggests that a useful (future) earthquake model might be simpler in some of its multiplicity of attributes than what most would want to believe.

There is another fascinating observation related to this set of curves. The red line corresponding to the day before the Mag 8 earthquake is significantly depressed in the frequency range from about 50 s to 4000 s. Could the depression of power at these long wavelengths be an indicator of an incipient earthquake? Only through the generation of data of this type, involving a significant number of large earthquakes, can there result an answer to this question.

The total power estimate in the range from 2.8 s to 6000 s corresponds to the longest-period-datum of the graph. Interestingly, this value is nearly constant for all days other than the day of the earthquake. In Fig. 16 these have been bar-graphed to show a possible interesting trend- before, during, and after the event.

Log of Total Power (period range 2 s to 6000 s) in W/kg

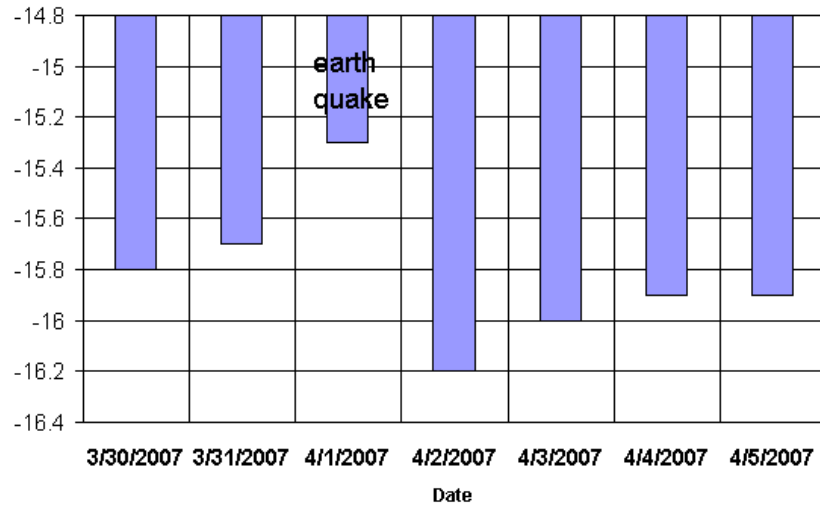


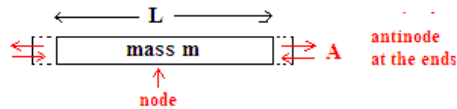
Figure 15. Bar-graph showing the trend of the peak values of the CSP for the five days of Fig. 14, along with two additional follow-on days.

11 Power of Eigenmode Oscillations

The eigenmode oscillations of the earth, also known as "free-oscillations" or "earth hum" are standing waves. We will now show that the power associated with a given one of these modes is identical to that of Eq.(10) except for a constant "shape factor" determined by the spherical harmonic (or tesseral harmonic) order number.

The physics of an oscillating sphere is much more complicated than the simple system that we choose here to analyze; however, the most important properties (dependence of power on frequency and amplitude) are identical for the systems. Shown in Fig. 16 is a homogeneous solid rod that is fixed at its center (a node) and excited into longitudinal vibration with the ends moving 180 degrees out of phase with respect to each other. This mode is a popular physics demonstration of standing waves in which the rod is made to "sing" loudly by means of friction stroking, through the use of violin bow rosin.

Example of standing wave energy--'Singing rod'



$$S(x,t) = A \sin(kx) \cos(\omega t), \quad k = \frac{2\pi}{\lambda}, \quad k \frac{L}{2} = \frac{\pi}{2}, \quad \text{so } k = \frac{\pi}{L}$$

$$u = \frac{\partial S}{\partial t} = -\omega A \sin\left(\frac{\pi}{L}x\right) \sin(\omega t)$$

$$dK = \frac{1}{2}(dm)u^2 = \frac{1}{2}(\mu dx)u^2 = \frac{1}{2}(\mu dx) \omega^2 A^2 \sin^2\left(\frac{\pi}{L}x\right) \cos^2(\omega t)$$

$$\langle dK(x) \rangle = \frac{1}{4}(\mu dx) \omega^2 A^2 \sin^2\left(\frac{\pi}{L}x\right)$$

$$\langle K \rangle = \frac{1}{2} \mu \omega^2 A^2 \int_0^{L/2} \sin^2\left(\frac{\pi}{L}x\right) dx = \frac{1}{8} m \omega^2 A^2$$

$$\langle E \rangle = \frac{1}{4} m \omega^2 A^2 \quad \longrightarrow \quad \boxed{\gamma m \omega^2 A^2 \text{ (general oscillator)}}$$

\longleftarrow shape factor

Figure 16. Example of a simple mechanical standing wave oscillation.

In the equations the brackets around a quantity indicate the time average of that harmonic quantity. The boxed result with the shape factor γ is valid for the description of the energy of a single mode of any mechanical standing wave, including the earth. More generally, the energy of any oscillation is quadratic in both the frequency and the amplitude. In the case of a waveguide, the amplitude would be that of the electric field. Notice also for this mechanical oscillator that the total energy of the mode is proportional to the total mass of system—a result which we will use in the conclusions section of this document.

The average power associated with the standing wave is obtained as before, by dividing the average energy expression in Fig. 16 by the period of oscillation. Ignoring the effect of finite Q that was part of earlier analysis, this yields the result:

$$\langle P \rangle = m \frac{\gamma}{2\pi} \omega^3 A^2 \quad (16)$$

In the "model" section of this VolksMeter manual is discussed the relative importance of tilt and acceleration on the response of a pendulum. At frequencies of the order of 1 mHz there is a "crossover" of sensitivity. At higher frequencies acceleration is dominant, whereas at lower frequencies tilt is dominant. Consider an eigenmode whose frequency is 1 mHz; for this case we can replace the A in Eq.(16) with the pendulum angular deflection θ_0 to yield the result:

$$\frac{\langle P \rangle}{m} \propto \frac{g^2 \theta_0^2}{2\pi f} \quad (17)$$

i.e., the average power divided by the mass of the earth (power per unit mass = 'specific' power) is the same as Eq. (10) apart from a multiplicative constant.

12 Conclusions concerning the PSD and the CSP

A natural conclusion is reached from the comparison of Eq.(17) to Eq. (10)—the specific power defined in this document "points meaningfully toward" the total oscillatory power of the earth in the period range specified by the specific power function. This "pointer" involves simply multiplying the PSD or the CSP values by 6×10^{24} kg.

This does not mean that precise estimates of vibrational power at a given frequency are yet possible, since there are too many uncertainties associated with quality factors and shape factors. But the fundamental physics of the matter is

clear-it should be possible to refine this approach for purpose of estimating global seismic power.

It is natural to question whether such a profound conclusion as this is possible, since the modelling is so simple compared to the enormous complexity of the earth in general. A point to keep in mind is that earthquake energies are routinely calculated, so why should not estimates of the quiescent global seismic power also be meaningful.

APPENDIX

Pendulum Dynamics

Free-body-diagram & equation of motion

Illustrated in Fig. P1 is one of the pendulums of the Volkmeter seismograph. For ease of drawing, the moving electrode array at the bottom (part of the SDC sensor) is shown with only four 'strips'; the actual instrument uses eight elements. Two cardinal points are indicated, the center of mass and the center of percussion. For horizontal motion of the instrument, acceleration applied at the axis yields a deflection of the opposite direction. Instantaneous rotation occurs about the center of percussion, which is located a distance $L_p = 29.5$ cm below the axis. The earth's field g acts at the center of mass, located the shorter distance $L = 20.6$ cm below the axis. For small deflections, the pendulum obeys the following equation of motion:

$$I \ddot{\theta} + I \frac{\omega_0}{Q} \dot{\theta} + M g L \theta = - \frac{I}{L_p} a(t) \quad (18)$$

where $M = 0.1628$ kg is the total mass, I is the moment of inertia about the axis, $Q = 0.8$ is the quality factor for the nearly critically damped instrument, and $a(t)$ is the time dependent horizontal acceleration of the earth.

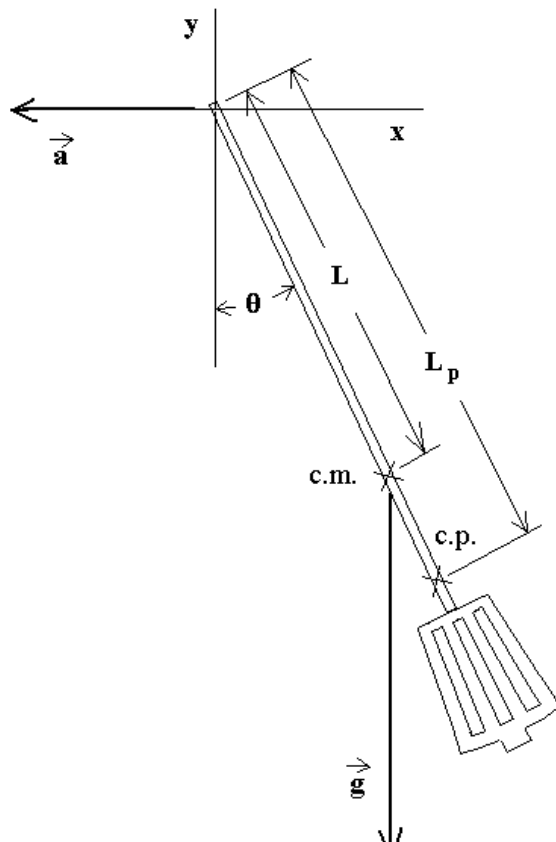




Figure P1. Free-body diagram to analyze the dynamics of the Volksmeter pendulum.

The natural (angular) frequency is given by

$$\omega_0 = \sqrt{\frac{M g L}{I_0 + M L^2}} = 5.768 \text{ s}^{-1} \quad (19)$$

that has used the parallel axis theorem; i.e., $I = I_0 + M L^2$, where $I_0 = 2.96 \times 10^{-3} \text{ kg m}^2$ is the moment of inertia about the center of mass.

Since the center of percussion obeys the relationship

$$L_P = \frac{I_0 + M L^2}{M L} \quad (20)$$

Eq. (1) reduces to

$$\ddot{\theta} + \frac{\omega_0}{Q} \dot{\theta} + \omega_0^2 \theta = -\frac{\omega_0^2}{g} a(t) \quad (21)$$

Although derived for a compound pendulum, Eq. (21) is of identical form to that of the simple pendulum; i.e., a point mass located at a distance L from the axis of rotation. The natural frequency of the compound pendulum is less, however; since the value of I_0 is not zero as in the case of the simple pendulum.

Transfer function

Horizontal acceleration

Consider the response of the pendulum when driven by horizontal ground motion, due to a non-zero acceleration $a(t)$ in Eq. (21). For harmonic ground motion at angular frequency ω and amplitude A , the pendulum responds according to

$$\left| \frac{\theta_0}{A} \right| = \frac{\omega_0^2}{g} \frac{\omega^2}{[(\omega_0^2 - \omega^2)^2 + \omega_0^2 \omega^2 / Q^2]^{1/2}} \quad (22)$$

where θ_0 is the amplitude in radians of the pendulum's steady state response.

Fig. P2 shows the 40 dB per decade fall-off in amplitude sensitivity for drive frequencies below the natural frequency of 0.918 Hz.

Bode plot of Volksmeter pendulum response to horizontal harmonic ground motion of amplitude A

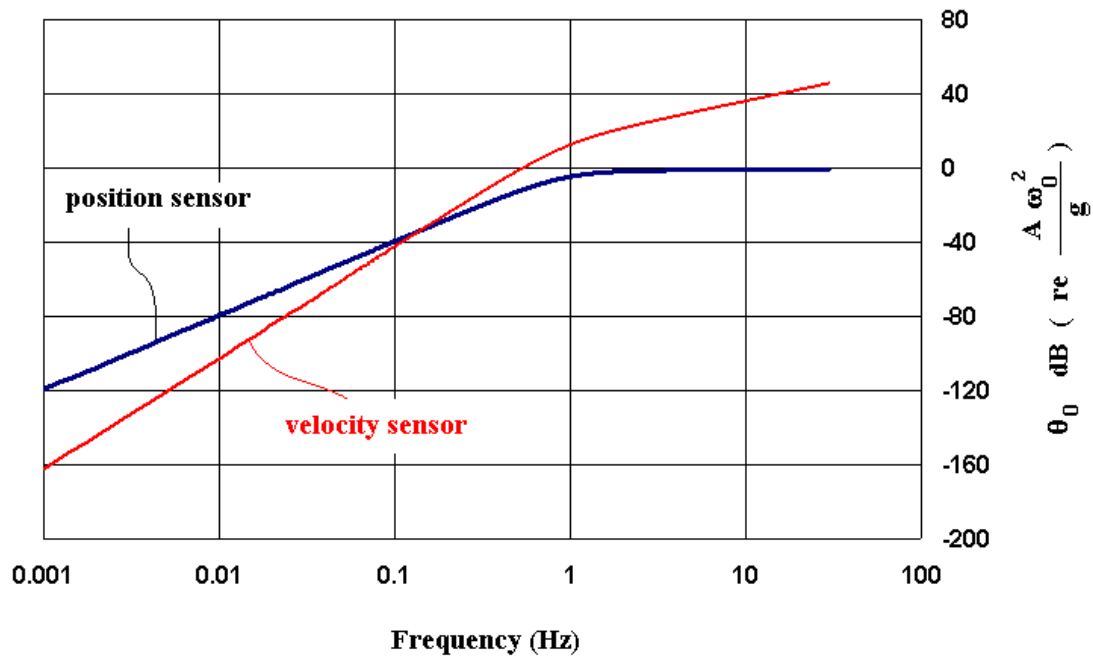


Figure P2. Decibel Plot (20 times the log to the base 10) of the ratio of pendulum amplitude to drive amplitude as a function of drive frequency.

Although the Volksmeter uses only a position sensor, Fig. P2 also shows (in red) the Bode plot that would result if a velocity sensor were instead used. The faster fall-off when using the velocity sensor is cause for a serious reduction in low-frequency performance. Elsewhere this performance degradation is quantified using calculations of the noise equivalent power spectral density.

Tilt Response

Unlike the pendulum's response to acceleration, which falls-off for drive frequency below the natural frequency in accord with Fig. P2 above; the tilt response of the pendulum is independent of frequency in the same range when using a position sensor.

The tilt component of the pendulum response is insignificant in the case of typical Earthquake waves. On the other hand, the pendulum responds primarily to tilt in the case of eigenmode oscillations. The first serious consideration of these characteristics of horizontal seismometers appears to have been the analyses by Rodgers [1]. To understand the physics involved, consider Fig. P3.

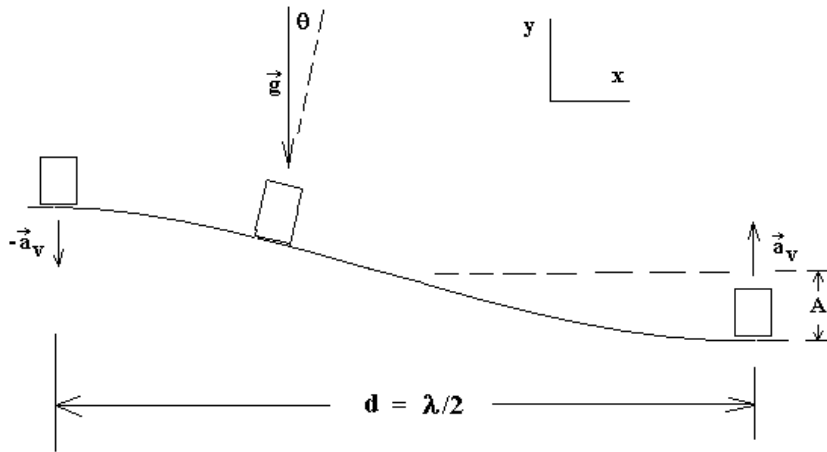


Figure P3. `Snapshot' of a transverse traveling wave of amplitude A . This constant-time graph of the wave is used to understand the response differences of a pendulum to (i) acceleration, and (ii) tilt. The distance d corresponds to one-half a wavelength λ .

The equation of a transverse harmonic traveling wave is given by

$$y(x,t) = A \sin(kx - \omega t) \quad (23)$$

where the wave number $k = 2\pi/\lambda = \omega/v$ is the ratio of the angular frequency to the magnitude of the phase velocity. For surface waves, typically $v \approx 3000$ m/s.

The vertical acceleration at any position x is given by

$$a(t)|_x = \frac{\partial^2 y(x,t)}{\partial t^2} = -\omega^2 y(x,t) \rightarrow |a_{\max}| = \omega^2 A \quad (24)$$

If the wave were purely transverse with vertical polarity as shown above, there would be no horizontal ground motion and thus no horizontal component of acceleration. The surface waves from distant earthquakes may be either Love waves with transverse, horizontally polarized motion or Rayleigh waves in which the ground moves in retrograde elliptical orbits. Only the latter will have a component of tilt. Typically, the vertical motion is 1.5 times the horizontal motion.

The response of the seismometer is consequently obtained by combining Eq.(24) with Eq.(21) and multiplying by a factor of $1/1.5$. Since tilt is important only at frequencies for which $\omega \ll \omega_0$, this results in

$$|\theta_0|_{\text{accel}} = \frac{\omega^2 A}{1.5 g} \quad (25)$$

The tilt of the instrument at a spatial point also varies harmonically in time and is specified (since $A \ll \lambda$) by

$$\theta(t)|_x = \frac{\partial y(x,t)}{\partial x} \rightarrow |\theta_{\max}| = |\theta_0|_{\text{tilt}} = kA = \frac{\omega}{v} A \quad (26)$$

Because the acceleration response is proportional at long periods to frequency to the second power, whereas tilt response is directly proportional to frequency; a place is reached as frequency is reduced-where a crossover occurs. The previously unimportant tilt component starts then to become the dominant component. To determine where this happens, we divide Eq.(26) by Eq.(25) to obtain the response ratio (tilt to acceleration) as

$$\rho = \frac{(1.5)g}{\omega v} \rightarrow 1 \text{ at crossover} \quad (27)$$

The ratio of vertical to horizontal amplitudes of Rayleigh particle motion is not constant, but rather depends on frequency. Just as there is a dispersive property to the velocity of propagation, so there is also dispersion associated with the particle motion. It is not therefore possible to predict a well-defined crossover frequency at which $\rho = 1$. If we assume a constant 1.5 in Eq.(27) for all wave speeds between 2 km/s and 4.2 km/s, then the following conclusion results:

For a conventional pendulum such as the Volkmeter, tilt response and acceleration response should be equally significant ($\rho = 1$) at a frequency in the range from 1.2 mHz to 0.53 mHz. i.e., in the range of frequencies of the lower eigenmodes.

Instead of being traveling waves, the eigenmode oscillations are standing waves, as illustrated in Fig. P4. The plots of this figure were generated from the equations modelled by Trefil in his text dealing with the physics of fluids and solids [2].

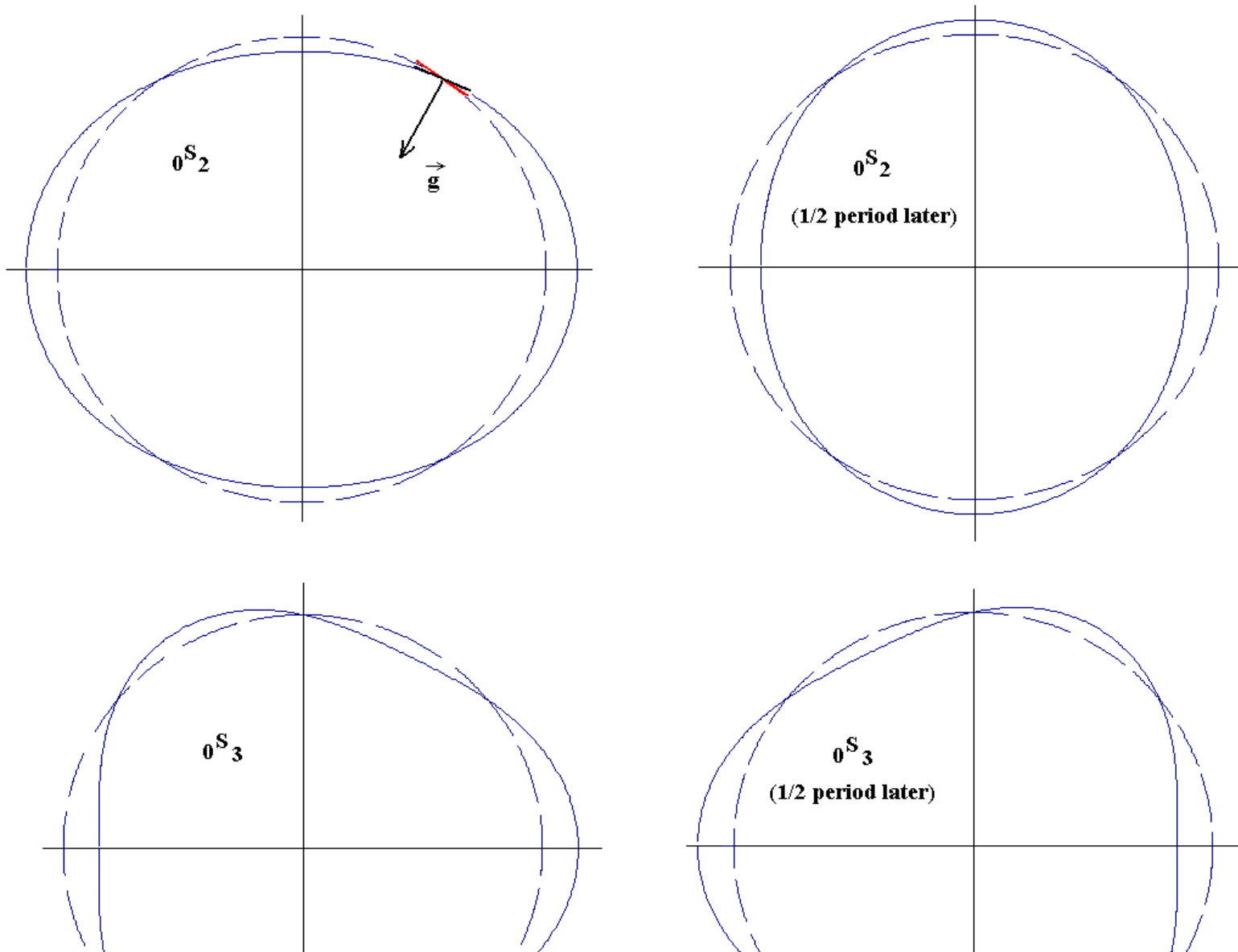




Figure P4. Illustration of pendulum tilt response to earth eigenmode oscillations. The direction of the earth's field does not vary appreciably during oscillation; therefore, the tilt is due to variations in the local horizon from one half-period to the next (refer to the bold tangent lines, upper left figure).

Rodgers [1] makes the claim that "...the principal response to the low-order spheroidal modes is as a tiltmeter". From the previously estimated range of values for the crossover; i.e., from 1.2 mHz to 0.53 mHz, we thus conclude that the highest frequency of 1.2 mHz is the better estimate.

Some Final Comments

About Eigenmode Oscillations

It is well known that the vast majority of the earth's natural oscillations are not highly monochromatic. Stated differently, they do not persist for hundreds or thousands of cycles. The one place where this rule does not apply is in the case of free-oscillations following huge earthquakes. A frequency regime where coherence time is significantly longer than elsewhere on a quasi-continuous basis is that of the primary and secondary microseisms, which typically last no more than tens of cycles. There is no physical basis for the belief that eigenmode oscillations with lifetimes of the order of tens of cycles should not also be observable on a fairly regular basis. Unfortunately, few instruments other than the VolksMeter (along with their associated data processing tools) are well suited to looking at these signals. This type of "free-oscillation" was first observed by accident during the course of solid-state physics experiments devoted to the study of chemisorbed gases on metallic surfaces [3]. The amplitudes of these modes can be significantly larger than the highly coherent signals excited by large earthquakes [4]. They have probably been routinely observed by others and classified erroneously as 'noise'. They show up easily in tiltmeter data by means of autocorrelation analysis [5].

Nonlinearities

All of the analyses considered for the generation of this manual assume that the instrument is adequately described by mathematics that derive from linear approximations. Much of the career of the author has been devoted to the study of both elastic anharmonicity and damping anharmonicity [6]. Whereas features of the elastic type have been routinely discussed in the literature of seismology, nothing of the damping type has ever been published there. Some of the author's work that is relevant to the performance of seismometers is to be found on (i) Mercer University webpages [7], and (ii) Cornell University's arxiv [8].

Bibliography

- (1) P. W. Rodgers, *The response of the horizontal pendulum seismometer to Rayleigh and Love waves, tilt, and free oscillations of the earth*, Bull. Seis. Soc. Amer., v. 58, no. 4, pp. 1385-1406 (1968).
- (2) J. S. Trefil, **Introduction to the Physics of Fluids and Solids**, Pergamon Press, p. 106 (1975).
- (3) Part of the PhD dissertation of M. H. Kwon (advisor Randall D. Peters), titled "Refinements of a new balance for measuring small force changes", Texas Tech University, December 1990. A journal paper concerned with the free-oscillations part of this dissertation was subsequently published: M. Kwon & R. Peters, "The study of eigenmode types and source nonlinearity in the free earth oscillations", Saemulli Vol. 35 no. 4, 569 (1995).
- (4) C. Braitenberg & M. Zadro, "Comparative analysis of the free oscillations generated by the Sumatra-Andaman Islands 2004 and the Chile 1960 Earthquakes", Bull. Seism. Soc. Amer., Vol 97, No. 1A, pp. S6-S17, Jan. 2007.
- (5) R. D. Peters, "Autocorrelation analysis of data from a novel tiltmeter, Fall Amer. Geophys. Union Conf., San Francisco (2000).
- (6) Articles by R. Peters in the 10th Ed. of the McGraw Hill Encyclopedia of Science and Technology: (i) Math. methods of *Chaos* in Physics, and (ii) the Anharmonic Oscillator. The curriculum vitae at the website of the next reference includes numerous other publications that relate either directly or indirectly to such matters.
- (7) <http://physics.mercer.edu/hpage/peters.html>
- (8) http://arxiv.org/find/physics/1/au:+Peters_R/0/1/0/all/0/1

File translated from T_EX by T_TH, version 1.95.

On 16 Apr 2007, 16:41.